

Minimizing the Levelized Cost of Energy in Single-Phase Photovoltaic Systems with an Absolute Active Power Control

Yang, Yongheng; Koutroulis, Eftichios; Sangwongwanich, Ariya; Blaabjerg, Frede

Published in:

Proceedings of the 2015 IEEE Energy Conversion Congress and Exposition (ECCE)

DOI (link to publication from Publisher):

[10.1109/ECCE.2015.7309665](https://doi.org/10.1109/ECCE.2015.7309665)

Publication date:

2015

Document Version

Early version, also known as pre-print

[Link to publication from Aalborg University](#)

Citation for published version (APA):

Yang, Y., Koutroulis, E., Sangwongwanich, A., & Blaabjerg, F. (2015). Minimizing the Levelized Cost of Energy in Single-Phase Photovoltaic Systems with an Absolute Active Power Control. In *Proceedings of the 2015 IEEE Energy Conversion Congress and Exposition (ECCE)* (pp. 28-34). IEEE Press.
<https://doi.org/10.1109/ECCE.2015.7309665>

General rights

Copyright and moral rights for the publications made accessible in the public portal are retained by the authors and/or other copyright owners and it is a condition of accessing publications that users recognise and abide by the legal requirements associated with these rights.

- Users may download and print one copy of any publication from the public portal for the purpose of private study or research.
- You may not further distribute the material or use it for any profit-making activity or commercial gain
- You may freely distribute the URL identifying the publication in the public portal -

Take down policy

If you believe that this document breaches copyright please contact us at vbn@aub.aau.dk providing details, and we will remove access to the work immediately and investigate your claim.

Minimizing the Levelized Cost of Energy in Single-Phase Photovoltaic Systems with an Absolute Active Power Control

Yongheng Yang^{†1}, *IEEE Member*, Eftichios Koutroulis^{‡2}, *IEEE Member*, Ariya Sangwongwanich^{†3},
and Frede Blaabjerg^{†4}, *IEEE Fellow*

[†]Department of Energy Technology
Aalborg University

Aalborg, DK-9220 Denmark

¹yoy@et.aau.dk; ³ars@et.aau.dk; ⁴fbj@et.aau.dk

[‡]School of Electronic and Computer Engineering
Technical University of Crete

Chania, GR-73100 Greece

²efkout@electronics.tuc.gr

Abstract—Several countries with considerable PhotoVoltaic (PV) installations are facing a challenge of overloading the power infrastructure during peak-power production hours. Regulations have been imposed on the PV systems, where more active power control should be flexibly performed. As an advanced control strategy, the Absolute Active Power Control (AAPC) can effectively solve the overloading issues by limiting the maximum possible PV power to a certain level (i.e., the power limitation), and also benefit the inverter reliability. However, its feasibility is challenged by the energy loss. An increase of the inverter lifetime and a reduction of the energy yield can alter the cost of energy, demanding an optimization of the power limitation. Therefore, aiming at minimizing the Levelized Cost of Energy (LCOE), the power limit is optimized for the AAPC strategy in this paper. The optimization method is demonstrated on a 3-kW single-phase PV system considering a real-field mission profile (i.e., solar irradiance and ambient temperature). The optimization results have revealed that superior performance in terms of LCOE and energy production can be obtained by enabling the AAPC strategy, compared to the conventional PV inverter operating only in the maximum power point tracking mode. In the presented case study, the minimum of LCOE is achieved for the system when the power limit is optimized to a certain level of the designed maximum feed-in power (i.e., 3 kW). In addition, the proposed LCOE-based analysis method can be used in the design of PV inverters considering mission profiles.

I. INTRODUCTION

Solar PhotoVoltaic (PV) installations are still at a spectacular growth rate worldwide [1], and thus challenging issues like overloading of the distributed grid due to peak power generation of PV systems appear occasionally [2], [3]. In the case of a large-scale adoption of PV systems, advanced control strategies, e.g., power-ramp control and absolute power control, which are currently required for wind power systems in different countries, should also be strengthened into PV systems [3]–[6]. Referring to the Absolute Active Power Control (AAPC) in the Danish grid code [5], a constant power generation control concept for PV systems by limiting the maximum feed-in power has been proposed in [4] in order to solve the overloading issues in peak-power production periods.

Compared to the solutions of expanding the grid capacity and integrating energy storage systems to tolerate the peak power, the AAPC scheme is a feasible and cost-effective strategy [7]–[11]. Hence, such a flexible active power control is gaining much awareness and also has already been put into effectiveness in some countries like Germany and Japan.

The AAPC viability in PV applications has been investigated in [4] and [9] in terms of a rough estimation of the energy losses and also the PV inverter lifetime, respectively. First, it has been found that the CPG control method with a reasonable power limitation (e.g., 80%) would not annually lead to a substantial energy yield reduction [3], [4]. In addition, the AAPC strategy allows a reduction of the thermal stresses on the power devices (e.g. IGBTs), since the power losses inducing temperature rises will be changed, when the PV system enters into the AAPC mode from Maximum Power Point Tracking (MPPT) mode and reversely. As a consequence, a hybrid control method (MPPT-AAPC) will also contribute to improved reliability and thereby extended lifetime of the PV system beyond solving the overloading issues [9].

Notably, both the energy production and the system lifetime are main indicators of the Levelized Cost Of Energy (LCOE), which has become the key to increase the competitiveness of the PV systems with other renewables [12], [13]. Thus, many efforts have been devoted into the design and control of PV systems with a common goal to reduce the cost of energy (i.e., lower LCOE). Means like adopting highly efficient transformerless PV inverters and reliability-oriented design have been witnessed in recent applications [14]–[20]. An adoption of the transformerless PV inverters can somehow increase the energy production due to their high efficiency [19]. However, the MPPT-AAPC operational mode is against the objective of maximizing the energy production of the PV systems, although the "capped" energy is quite limited throughout a year. Whilst the improved reliability (i.e., extended service time of the PV systems) can compensate for such a loss to some extent as long as the power limitation is appropriately designed.

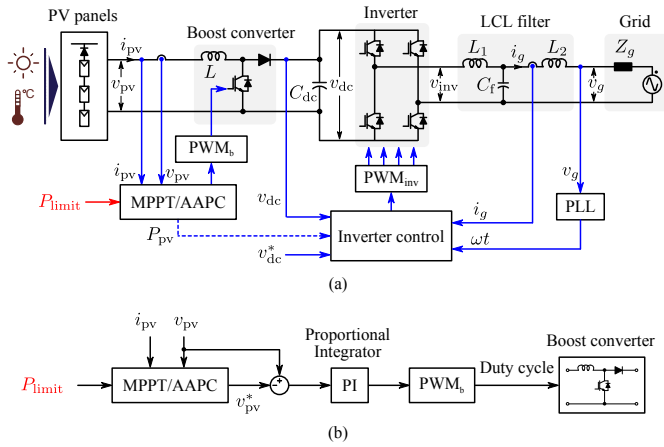


Fig. 1. A single-phase double-stage grid-connected PV system with an LCL filter: (a) hardware schematic and overall control structure and (b) control block diagram of the boost converter with the Absolute Active Power Control (AAPC) scheme.

Thus, this paper serves to find the optimal power limitation level for the MPPT-AAPC scheme with a target of minimizing the LCOE considering long-term mission profiles (i.e., solar irradiance and ambient temperature). In order to optimize the power limitation, a mission-profile-based analysis approach is introduced, as well as the control principle in § II. As it is illustrated in § III, the obtained temperature loading profiles and power losses offer the possibility to quantitatively calculate the LCOE of the PV inverter under a given mission profile, while also is considered the PV inverter reliability. Then, case studies on a 3-kW single-phase grid-connected PV system with the MPPT-AAPC control using different power limitations have been presented in § IV. The analysis of LCOE presented in this paper can also be adopted in the optimal design of future PV inverters considering the mission profiles. Finally, concluding remarks are given in § V.

II. ABSOLUTE ACTIVE POWER CONTROL

A. Absolute Active Power Control (AAPC)

Fig. 1 shows the configuration of a double-stage PV system with a hybrid power control and a general control structure of the boost converter stage. Although there are several AAPC possibilities to achieve a constant power generation when the available PV power, P_{pv} , exceeds the power limit, P_{limit} , a solution by modifying the MPPT control has been adopted from the viewpoint of simplicity. It can be observed in Fig. 1 that the AAPC scheme is implemented in the control of the boost converter. As aforementioned, the PV inverter can be transformerless to maintain a high efficiency, and thus a full-bridge topology with a bipolar modulation scheme is adopted in Fig. 1.

In respect to the AAPC scheme employed in this paper, the operation principle of a PV system with the hybrid control scheme (MPPT-AAPC) can be described as follows. When the available PV output power P_{pv} exceeds the power limitation P_{limit} , the system goes into the AAPC mode. In that case, the

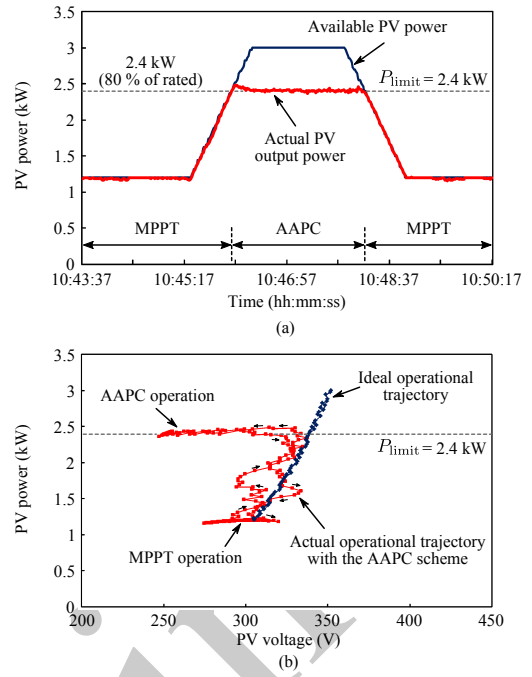


Fig. 2. Operation example (experiments) of a 3-kW single-phase double-stage PV system with the Absolute Active Power Control (AAPC) scheme, where the power limit is set to be 80 % of the rated power (i.e., $P_{limit} = 2.4$ kW) and the ambient temperature is 25 °C: (a) PV output power and (b) operational trajectories.

PV output reference voltage v_{pv}^* is continuously “perturbed” towards certain points, at which a constant power generation of the PV panels is achieved. While once $P_{pv} \leq P_{limit}$, the PV system operates in the MPPT mode with a peak power injecting to the grid from the PV panels (i.e., the energy harvesting is maximized). In both modes, a Proportional Integrator (PI) controller is employed to regulate the PV output voltage v_{pv} through controlling the boost converter. Fig. 2 demonstrates the performance of a 3-kW single-phase double-stage PV system with the MPPT-AAPC scheme under a trapezoidal solar profile. It can be observed in Fig. 2 that the adopted control scheme (Fig. 1(b)) can effectively attain a constant power production as well as smooth and stable operation mode transients. It should be pointed out that the operating point in the AAPC mode was controlled at the left-side of the maximum power point in Fig. 2. However, it can also operate at the right-side of the maximum power point at the cost of increased power losses [4]. Moreover, the PV system may go into instability in that case. Hence, in this paper, the AAPC operating point is regulated at the left-side of the maximum power point.

B. Mission Profile Translation

A mission profile is normally referred to as a simplified representation of relevant conditions under which the considered system is operating [21]–[23]. For the grid-connected PV systems, the mission profile includes the solar irradiance and the ambient temperature of certain locations, where the PV systems were installed, and it can be taken as a reflection

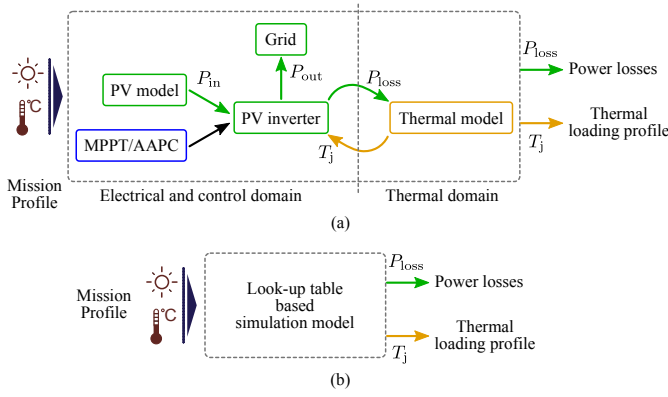


Fig. 3. Approach to translate mission profiles to power losses P_{loss} and thermal loading (i.e., device junction temperature T_j): (a) for short-term mission profiles and (b) for long-term mission profiles.

of the intermittent nature of the solar PV energy. Thus, the mission profile becomes an essential part for the PV inverter reliability analysis. Specifically, in order to perform the reliability analysis of the PV inverter, it is inevitable to translate the mission profile to the power losses and the thermal loading in a long-term operation (e.g., a year operational profile) [19]–[21], [24], [25].

Fig. 3 illustrates the mission profile translation approach, with which the power losses and thermal loading of the power devices under any given mission profile can be obtained. Notably, a number of cases under constant environmental conditions (e.g., ambient temperature: 25 °C and solar irradiance: 1000 W/m²) has been done according to Fig. 3(a) in order to build up the look-up table based loss and thermal models. Subsequently, a long-term mission profile with a high sampling rate are directly translated to the total power losses (and also energy production) as well as the thermal loading of the power devices, which are then used for LCOE analysis in the following sections.

III. LEVELIZED COST OF ENERGY (LCOE) OF PV INVERTERS

The PV inverter LCOE (€/Wh) is a function of the PV inverter power rating denoted as P_r [12], [14]. It can be expressed as

$$\text{LCOE}(P_r) = \frac{C_{\text{inv}}(P_r)}{E_y(P_r)} \quad (1)$$

in which $C_{\text{inv}}(\cdot)$ (€) is the present total cost of PV inverter during its lifetime and $E_y(\cdot)$ (Wh) is the total energy injected into the grid by the PV inverter during its life span. In the case that the PV inverter operates in the AAPC mode, its nominal power rating is constrained to $P_r = P_{\text{limit}}$ as discussed in § II.A, while in the MPPT mode it holds that $P_r = P_n$, with P_n being the inverter nominal power. Namely, in the MPPT mode, the input power of the inverter is curtailed at P_n (i.e., the PV inverter is normally slightly under-designed), while in the AAPC mode the curtailment limit is equal to P_{limit} (i.e., to maintain a constant power production).

In (1), the present total cost of the PV inverter depends on the corresponding manufacturing and maintenance costs [14]

$$C_{\text{inv}}(P_r) = C_m(P_r) + M_c(P_r) \quad (2)$$

where $C_m(\cdot)$ (€) is the PV inverter manufacturing cost and $M_c(P_r)$ (€) is the present value of the total maintenance cost of the PV inverter through its lifetime. Furthermore, the PV inverter manufacturing cost is proportional to P_r :

$$C_m(P_r) = c_m P_r + C_0 \quad (3)$$

with c_m being the proportionality factor (€/kW) and C_0 being the initial cost, which has been considered as zero in this paper since it is much lower than the total cost of the PV inverter.

As a consequence, in the AAPC mode, the PV inverter cost is proportional to the power limit P_{limit} , while in the MPPT mode the inverter cost is proportional to the nominal power rating P_n . The total maintenance cost, $M_c(\cdot)$, depends on the PV inverter reliability features, which in turn depends on the power rating of the PV inverter. In the proposed methodology, the lifetime (in years) of the PV inverter power devices are initially calculated. It is assumed that each time when the end-of-life of the PV inverter power devices is reached, the maintenance of the PV inverter will be performed, imposing the corresponding maintenance cost. Therefore, the present value of the total maintenance cost of the PV inverter, $M_c(P_r)$, is calculated by reducing the (future) expenses occurring at the end of the power devices lifetime for repairing the PV inverter to the corresponding present value, as follows:

$$M_c(P_r) = \sum_{j=1}^n LF_j(P_r) \cdot R_c \cdot P_r \cdot \frac{(1+g)^j}{(1+d)^j} \quad (4)$$

where n is the PV system operational lifetime (e.g., 30 years), R_c (€/kW) is the present value of the PV inverter repairing cost per kW of the power rating, g (%) is the annual inflation rate, d (%) is the annual discount rate, and $LF_j(\cdot)$ is the inverter lifetime with $1 \leq j \leq n$. If the lifetime of the power devices expires at the j -th year of operation, $LF_j(P_n) = 1$; otherwise, $LF_j(P_n) = 0$. Notably, the repairing cost R_c in (4) consists of both the purchase cost of the failed power devices, as well as the potential labor and transportation expenses for repairing/replacing the PV inverter. The above discussion has confirmed that the AAPC control method will affect the LCOE (i.e., the cost of PV energy).

It should be pointed out that the following demonstrates how to calculate the LCOE of only the PV inverter (as shown in (1)) considering the long-term mission profile effect on the inverter lifetime, where the grid fundamental-frequency thermal cycles are not considered at this stage. However, the PV panel cost also accounts for a major share of the total cost of the entire grid-connected PV system [12], [14], where it also includes other components like capacitors and Print Circuit Boards (PCB) for implementing the control algorithms. This becomes the main limitation of the presented LCOE optimization method, and it will affect the design results. Nevertheless, the LCOE analysis approach and also the optimization of the

TABLE I

PARAMETERS OF THE BP 365 SOLAR PV PANEL AT STANDARD TEST CONDITIONS (1000 W/m², AM 1.5 G, 25 °C).

Parameter	Symbol	Value
Rated power	P_{mpp}	65 W
Voltage at P_{mpp}	V_{mpp}	17.6 V
Current at P_{mpp}	I_{mpp}	3.69 A
Open-circuit voltage	V_{oc}	21.7 V
Short-circuit current	I_{sc}	3.99 A

TABLE II

PARAMETERS OF THE SINGLE-PHASE DOUBLE-STAGE GRID-CONNECTED PV SYSTEM SHOWN IN FIG. 1.

Parameter	Symbol	Value
Grid voltage amplitude	v_{gn}	325 V
Grid frequency	ω_0	$2\pi \times 50$ rad/s
Boost converter inductor	L	5 mH
DC-link capacitor	C_{dc}	2200 μ F
Grid impedance	L_g	2 mH
	R_g	0.2 Ω
LCL filter	L_1, L_2	2 mH, 3 mH
	C_f	4.7 μ F
Sampling frequency	f_{sw}	10 kHz
Switching frequencies for both converters	f_b, f_{inv}	10 kHz

AAPC control power limitation can be of much value to assess and design of multiple PV systems.

IV. MINIMIZED LCOE (CASE STUDY RESULTS)

A. System Description

The LCOE analysis approach has been applied for the optimal design of a PV inverter with a nominal power equal to $P_n = 3$ kW and also the AAPC capability. The PV system lifetime has been set to $n = 30$ years, while the financial and economic performances of the PV inverter in the AAPC and MPPT modes, respectively, have been investigated by applying the following values in (1)-(4): $c_m = 200$ €/kW, $R_c = 200$ €/kW, $g = 2$ % and $d = 5$ %. A mission profile shown in Fig. 4 with a sampling rate of 1 sample/min has been used. The BP 365 PV panel [26] is adopted in the case studies. Parameters of the PV panel are given in Table I. Three PV strings are connected in parallel to the boost converter, and each string consists of 15 PV panels in series. Thus, the rated maximum power P_{max} is around 3 kW. The other system parameters are given in Table II. Studies are then conducted according to Figs. 1 and 3. The effectiveness of the mission profile translation approach (Fig. 3) is demonstrated by the resultant thermal loading profiles presented in Fig. 5, which indicates that the junction temperature is reduced by the AAPC scheme. Hence, the PV inverter lifetime may be improved.

B. LCOE Analysis

According to the mission profile translation approach, the thermal loading as well as the power losses can be obtained. Consequently, the lifetime enabled by a rainflow counting algorithm [27]–[29] and the energy yield can be calculated under different power limits P_{limit} .

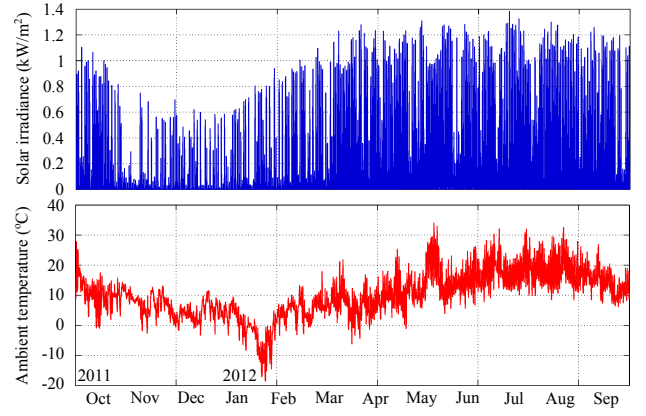


Fig. 4. A real-field yearly mission profile for a 3-kW grid-connected PV system with the absolute active power control: (a) solar irradiance and (b) ambient temperature.

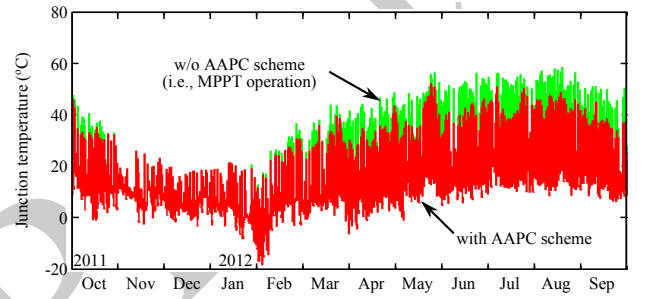


Fig. 5. Thermal loading of the power devices of the PV inverter with and without the absolute active power control ($P_{limit} = 2.4$ kW, i.e., 80 % of the nominal power) under the yearly real-field mission profile (Fig. 4).

The energy production of the PV inverter in the AAPC mode for various values of P_{limit} is illustrated in Fig. 6, where the energy production has been normalized to the corresponding energy production in the MPPT mode. Due to the limitation of feed-in power imposed by the converter control in the AAPC mode, the resultant energy production shown in Fig. 6 is lower than that in the MPPT mode for $P_{limit} = 0$ –110 % of the rated power P_n . However, in the case that P_{limit} is higher than 120 %, then the energy production in the AAPC mode is higher than that produced only in the MPPT mode, where the input power of the inverter is curtailed at the designed power rating P_n , as it can be observed in Fig. 6. This is because the PV panel rating has been selected to be equal to 3 kW at 1000 W/m² solar irradiance and 25 °C ambient temperature. Since the mission profile shown in Fig. 4 has some periods where the solar irradiance is higher than 1000 W/m², the power production during those periods is higher than designed power rating P_n , which is also the curtailment limitation in the MPPT mode. Thus, during those time intervals, the excess energy is lost when even operating in the MPPT mode.

The lifetime of the PV inverter when operating in the AAPC mode for various values of the power limitation P_{limit} , is presented in Fig. 7. It is observed in Fig. 7 that for $P_{limit} = 0$ –100 %, the PV inverter lifetime is higher than the operational lifetime of the PV system, thus guaranteeing that no failures

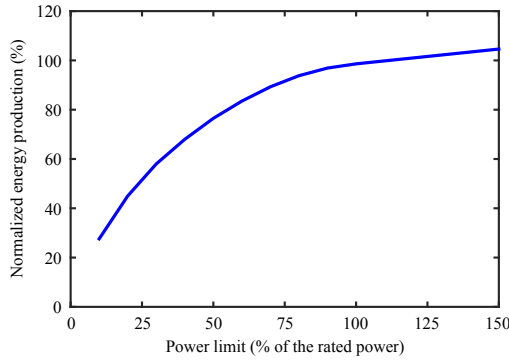


Fig. 6. Energy production of the 3-kW single-phase PV system in the MPPT-AAPC mode according to the mission profile shown in Fig. 4, which has been normalized to the corresponding energy production only in the MPPT mode, for various values of the power limit P_{limit} .

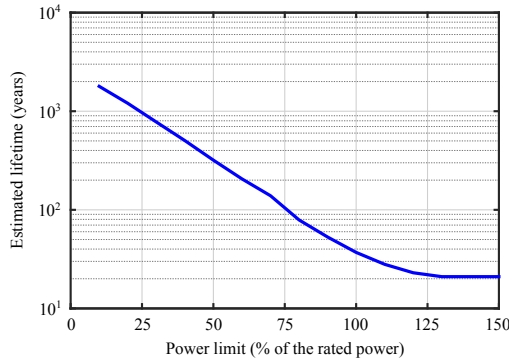


Fig. 7. Lifetime of the 3-kW single-phase PV inverter when operating in the MPPT-AAPC mode for various power limits P_{limit} considering the mission profile effect (the mission profile shown in Fig. 4 has been used).

of the power devices will occur during that period. The corresponding present value of the lifetime maintenance cost in the AAPC mode for various values of the power limitation P_{limit} , is shown in Fig. 8. When the power limit P_{limit} reaches the range of 100-150 % of the rated power, the PV inverter lifetime in the AAPC mode is progressively reduced to around 21 years, corresponding to one repair of the PV inverter during the PV system lifetime and the maintenance cost is increased accordingly to (4). In contrast, the PV inverter lifetime in the MPPT mode is around 21 years, resulting in one inverter repair during the lifetime of the PV system, which corresponds to $M_c = 326.4$ €.

The total cost of the PV inverter operating in the MPPT-AAPC mode, including the manufacturing and maintenance expenses according to (2), is plotted in Fig. 9. For values of the power limit P_{limit} in the range of 0-100 % of the rated power, the maintenance cost is zero, as it is shown in Fig. 8. Hence, the total cost depends only on the inverter construction cost, which is proportional to the power limit P_{limit} according to (3). However, when $P_{\text{limit}} > 100$ %, the total cost in the MPPT-AAPC mode is affected by both the construction and the maintenance expenses, as indicated in Fig. 9. In the MPPT mode, the total cost of the inverter is equal to $C_{\text{inv}} = 926.4$ €.

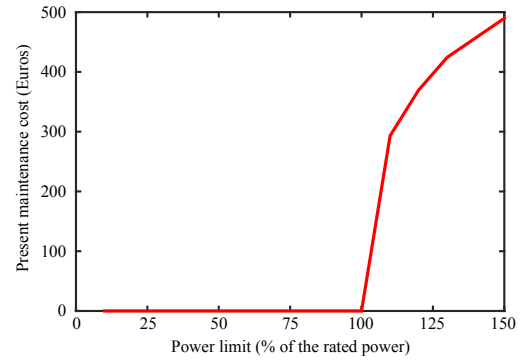


Fig. 8. Present value of the lifetime maintenance cost of the 3-kW single-phase PV inverter when operating in the MPPT-AAPC mode for various values of the power limit P_{limit} , considering the mission profile that has been presented in Fig. 4.

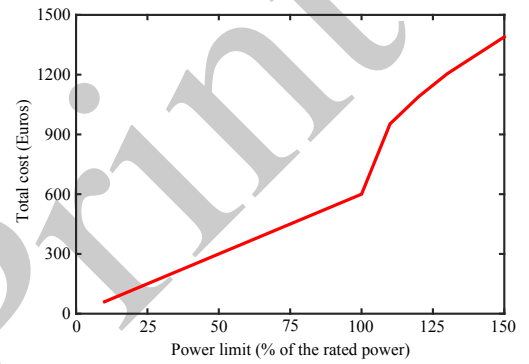


Fig. 9. Total cost of the 3-kW single-phase PV inverter operating in the MPPT-AAPC mode for various values of the power limit P_{limit} , where the mission profile shown in Fig. 4 has been used.

Although the lifetime energy production is higher in the MPPT mode, as it is analyzed above, the PV inverter cost is also higher in this operating mode when $P_{\text{limit}} > 100\%P_n$, as shown in Fig. 9.

Moreover, the LCOE of 3-kW PV inverter in the MPPT-AAPC and MPPT modes, respectively, have been calculated using (1) for various values of the power limit P_{limit} in order to find the optimal power limitation under this mission profile shown in Fig. 4. The results are presented in Fig. 10. It can be seen in Fig. 10 that the LCOE value in the MPPT-AAPC mode is always less than that in the only-MPPT mode (i.e., the conventional operational mode at unity power factor), but the energy production is also less in the case of the MPPT-AAPC operation, as it is discussed previously.

As a consequence, it was reasonably considered that in practical applications, in order to achieve a total energy generation which is equal to or higher than that in the MPPT mode, multiple identical PV inverters would be required to operate in parallel in the MPPT-AAPC mode, each of them having a feed-in power limitation of P_{limit} . The resultant value of the LCOE in the MPPT-AAPC mode, $\text{LCOE}_{n,e}(\cdot)$, has been calculated as (5). This LCOE has been normalized to the LCOE in the MPPT mode when producing an amount of

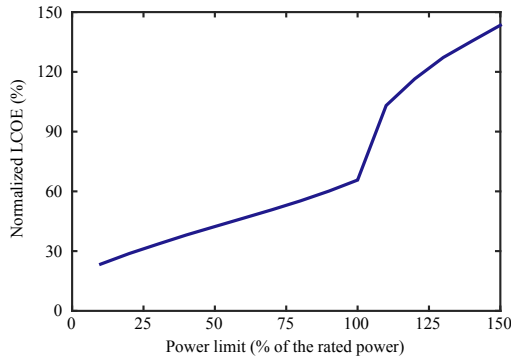


Fig. 10. LCOE of the 3-kW PV inverter system in the MPPT-AAPC mode normalized to the LCOE in the MPPT mode for various power limits P_{limit} , based on the mission profile shown in Fig. 4, where only the PV inverter is considered.

energy during the PV system lifetime, which is equal to or higher than that in the MPPT mode.

$$\text{LCOE}_{n,e}(P_{\text{limit}}) = \frac{\text{LCOE}_{\text{AAPC-MPPT}}(P_{\text{limit}})}{\text{LCOE}_{\text{MPPT}}(P_n)} \cdot N_{\text{inv}}(P_{\text{limit}}) \quad (5)$$

with

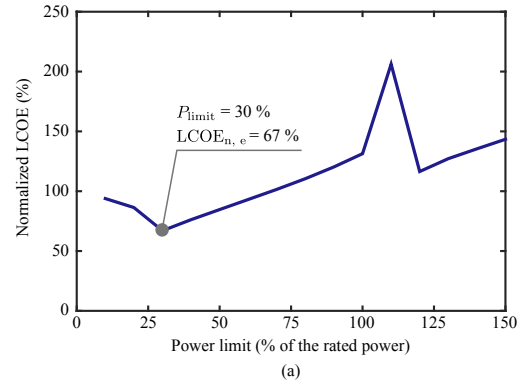
$$N_{\text{inv}}(P_{\text{limit}}) = \left\lceil \frac{E_{y, \text{MPPT}}(P_n)}{E_{y, \text{AAPC-MPPT}}(P_{\text{limit}})} \right\rceil \quad (6)$$

and $N_{\text{inv}}(\cdot)$ is the number of inverters, which must operate in parallel in the MPPT-AAPC mode for achieving a total energy generation. The total energy yield of $N_{\text{inv}}(\cdot)$ PV inverters should be equal to or higher than that produced in the MPPT mode. $\text{LCOE}_{\text{AAPC-MPPT}}(\cdot)$, $\text{LCOE}_{\text{MPPT}}(\cdot)$ are the LCOEs in the MPPT-AAPC and MPPT modes, respectively, and $E_{y, \text{MPPT}}(\cdot)$, $E_{y, \text{AAPC-MPPT}}(\cdot)$ are the corresponding lifetime energy productions. Then, the total energy production when employing $N_{\text{inv}}(\cdot)$ inverters in the MPPT-AAPC mode operating in parallel, is given by

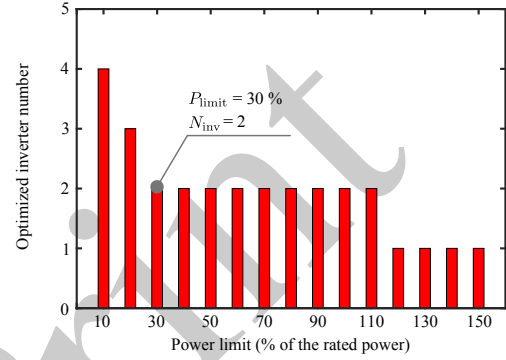
$$E_{\text{tn, AAPC - MPPT}}(P_{\text{limit}}) = N_{\text{inv}}(P_{\text{limit}}) \cdot \frac{E_{y, \text{AAPC - MPPT}}(P_{\text{limit}})}{E_{y, \text{MPPT}}(P_n)} \quad (7)$$

which is normalized to the energy production in the MPPT mode, $E_{\text{tn, AAPC-MPPT}}(\cdot)$.

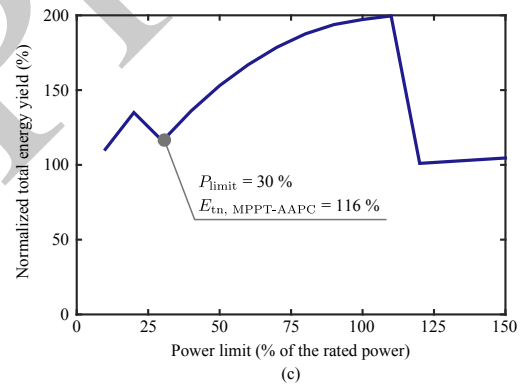
For various levels of the feed-in power limit, P_{limit} , the resultant values of $\text{LCOE}_{n,e}(\cdot)$, $N_{\text{inv}}(\cdot)$ and $E_{\text{tn, AAPC - MPPT}}(\cdot)$ are depicted in Fig. 11. The $\text{LCOE}_{n,e}(\cdot)$ function exhibits an overall minimum at $P_{\text{limit}} = 30\%$, which is equal to 67%. It means that the LCOE has been minimized. In that case, by employing two identical PV inverters with a feed-in limit of $P_{\text{limit}} = 30\%$ of the rated power for each, it will result in a reduction of the total PV inverter structure LCOE by 33% compared to using a single inverter unit operating only in the MPPT mode, as it can be observed in Fig. 11(b). Moreover, the total energy generated is simultaneously increased by 16% as it is shown in Fig. 11(c). In addition, the same process with $c_m = 300 \text{ €/kW}$ and $R_c = 80 \text{ €/kW}$ is applied to the PV inverter under the same mission profile, and it also contributes to the minimum of $\text{LCOE}_{n,e}(\cdot)$ at $P_{\text{limit}} = 30\%$.



(a)



(b)



(c)

Fig. 11. Optimized results for the 3-kW PV inverter systems with the MPPT-AAPC scheme for various levels of the feed-in power limit P_{limit} when only considering the cost of the PV inverters: (a) minimized $\text{LCOE}_{n,e}(\cdot)$, (b) optimized number of PV inverters in parallel N_{inv} , and (c) obtained total energy production $E_{\text{tn, MPPT-AAPC}}(\cdot)$.

In such a case, employing two inverters operating in parallel with $P_{\text{limit}} = 30\%$, the LCOE in the MPPT-AAPC mode is thus lowered by approximately 10%, and also the total energy production is increased by 16%, compared to the corresponding values obtained by a single PV inverter operating only in the MPPT mode.

However, as it has also been mentioned in § II, this paper only calculates the LCOE for the PV inverters, when the mission profile induced thermal cycles are considered. When the line-frequency thermal cycles are taken into account, the lifetime will be affected [9], [30]. At the same time, the LCOE in the MPPT-AAPC mode may be higher than that in the MPPT mode, if the cost of PV panels is counted in

according to (2). In that case, it is still possible to derive the optimal PV system configurations by mixing a low power PV inverter with a higher power one, both operating in the MPPT-AAPC mode, according to the presented optimization method. Similar objectives (minimized LCOE and maximized energy production) can then be reached.

V. CONCLUSION

The Levelized Cost Of Energy (LCOE) of PV inverters with an Absolute Active Power Control (AAPC) scheme has been calculated and analyzed in this paper in the consideration of a long-term real-field mission profile. The analysis has revealed that the hybrid power control (i.e., with the mixture of MPPT and AAPC operation modes, MPPT-AAPC) can contribute to an improved lifetime of the power devices due to the reduced thermal loading. However, a reduction of energy production is associated with this reliability benefit. In this paper, it has been demonstrated that by optimizing the power limit imposed on multiple PV inverters, which operate in the MPPT-AAPC mode, a reduction of LCOE (minimized) and, simultaneously, an increase of the PV generated energy are achieved, compared to the use of a single PV inverter, which operates only in the MPPT mode.

Most importantly, the presented optimization method and the LCOE analysis can be an effective design tool for PV system planning (e.g., a cluster of PV inverters), when the mission profile (both long-term and line-frequency thermal cycles) and the PV panel cost are also considered. Specifically, by applying the last part of the optimization design in this paper (i.e., related to Fig. 11), the operation of each individual inverter in the cluster of the PV systems can be optimally selected, in such a way that:

- 1) an overall constant power production is achieved,
- 2) the total energy production is not reduced, and
- 3) the LCOE is minimized.

REFERENCES

- [1] SolarPower Europe, "Global market outlook for solar power 2015 - 2019," European Photovoltaic Industry Association, Bruxelles, Tech. Rep., 2015. [Online]. Available: <http://www.solarpowereurope.org/>
- [2] D. Rosenwirth and K. Strubbe, "Integrating variable renewables as Germany expands its grid," *RenewableEnergyWorld.com*, Mar. 21, 2013. [Online]. Available: <http://www.renewableenergyworld.com>
- [3] Fraunhofer ISE, "Recent facts about photovoltaics in Germany," Fraunhofer Institute for Solar Energy Systems ISE, Germany, Tech. Rep., May 2015. [Online]. Available: <http://www.ise.fraunhofer.de>
- [4] Y. Yang, H. Wang, F. Blaabjerg, and T. Kerekes, "A hybrid power control concept for PV inverters with reduced thermal loading," *IEEE Trans. Power Electron.*, vol. 29, no. 12, pp. 6271–6275, Dec. 2014.
- [5] ENERGINET.DK, "Wind power plants with a power output greater than 11 kW," *Technical Regulation 3.2.5*, Sept. 2010.
- [6] M. Lang and A. Lang, "The 2014 German renewable energy sources act revision—from feed-in tariffs to direct marketing to competitive bidding," *Journal of Energy & Natural Resources Law*, vol. 33, no. 2, pp. 131–146, 2015.
- [7] T. Stetz, F. Marten, and M. Braun, "Improved low voltage grid-integration of photovoltaic systems in Germany," *IEEE Trans. Sustain. Energy*, vol. 4, no. 2, pp. 534–542, Apr. 2013.
- [8] H. Beltran, E. Bilbao, E. Belenguer, I. Etxeberria-Otadui, and P. Rodriguez, "Evaluation of storage energy requirements for constant production in PV power plants," *IEEE Trans. Ind. Electron.*, vol. 60, no. 3, pp. 1225–1234, Mar. 2013.
- [9] Y. Yang, H. Wang, and F. Blaabjerg, "Improved reliability of single-phase PV inverters by limiting the maximum feed-in power," in *Proc. of ECCE*, pp. 128–135, Sept. 2014.
- [10] A. Ahmed, L. Ran, S. Moon, and J.-H. Park, "A fast PV power tracking control algorithm with reduced power mode," *IEEE Trans. Energy Convers.*, vol. 28, no. 3, pp. 565–575, Sept. 2013.
- [11] A. Hoke and D. Maksimovic, "Active power control of photovoltaic power systems," in *Proc. of SusTech*, pp. 70–77, Aug. 2013.
- [12] Fraunhofer ISE, "Levelized cost of electricity-renewable energy technologies," Fraunhofer Institute for Solar Energy Systems ISE, Freiburg, Germany, Tech. Rep., Nov. 2013. [Online]. Available: <http://www.ise.fraunhofer.de>
- [13] Y. Xue, K.C. Divya, G. Griepentrog, M. Liviu, S. Suresh, and M. Manjrekar, "Towards next generation photovoltaic inverters," in *Proc. of ECCE*, pp. 2467–2474, Sept. 2011.
- [14] E. Koutroulis and F. Blaabjerg, "Design optimization of transformerless grid-connected PV inverters including reliability," *IEEE Trans. Power Electron.*, vol. 28, no. 1, pp. 325–335, Jan. 2013.
- [15] J.-Y. Chen, C.-H. Hung, J. Gilmore, J. Roesch, and W. Zhu, "LCOE reduction for megawatts PV system using efficient 500 kW transformerless inverter," in *Proc. of ECCE*, pp. 392–397, Sept. 2010.
- [16] S. Saridakis, E. Koutroulis, and F. Blaabjerg, "Optimization of SiC-based H5 and Conergy-NPC transformerless PV inverters," *IEEE J. Emerg. Sel. Top. Power Electron.*, vol. 3, no. 2, pp. 555–567, Jun. 2015.
- [17] Z. Moradi-Shahrbabak, A. Tabesh, and G.R. Yousefi, "Economic design of utility-scale photovoltaic power plants with optimum availability," *IEEE Trans. Ind. Electron.*, vol. 61, no. 7, pp. 3399–3406, Jul. 2014.
- [18] H. Wang, M. Liserre, F. Blaabjerg, P. de Place Rimmen, J.B. Jacobsen, T. Kvisgaard, and J. Landkildehus, "Transitioning to physics-of-failure as a reliability driver in power electronics," *IEEE J. Emerg. Sel. Top. Power Electron.*, vol. 2, no. 1, pp. 97–114, Mar. 2014.
- [19] Y. Yang, H. Wang, F. Blaabjerg, and K. Ma, "Mission profile based multi-disciplinary analysis of power modules in single-phase transformerless photovoltaic inverters," in *Proc. of EPE*, pp. 1–10, Sept. 2013.
- [20] N.-C. Sintamarean, F. Blaabjerg, H. Wang, F. Iannuzzo, and P. de Place Rimmen, "Reliability oriented design tool for the new generation of grid connected PV-inverters," *IEEE Trans. Power Electron.*, vol. 30, no. 5, pp. 2635–2644, May 2015.
- [21] D. Hirschmann, D. Tissen, S. Schroder, and R.W. De Doncker, "Reliability prediction for inverters in hybrid electrical vehicles," *IEEE Trans. Power Electron.*, vol. 22, no. 6, pp. 2511–2517, Nov. 2007.
- [22] M. Ciappa, "Lifetime prediction on the base of mission profiles," *Microelectronics reliability*, vol. 45, no. 9, pp. 1293–1298, 2005.
- [23] S.E. De Leon-Aldaco, H. Calleja, and J. Aguayo Alquicira, "Reliability and mission profiles of photovoltaic systems: a FIDES approach," *IEEE Trans. Power Electron.*, vol. 30, no. 5, pp. 2578–2586, May 2015.
- [24] M. Musallam, C. Yin, C. Bailey, and M. Johnson, "Mission profile-based reliability design and real-time life consumption estimation in power electronics," *IEEE Trans. Power Electron.*, vol. 30, no. 5, pp. 2601–2613, May 2015.
- [25] S.E. De León-Aldaco, H. Calleja, F. Chan, and H.R. Jiménez-Grajales, "Effect of the mission profile on the reliability of a power converter aimed at photovoltaic applications - a case study," *IEEE Trans. Power Electron.*, vol. 28, no. 6, pp. 2998–3007, Jun. 2013.
- [26] Plexim GmbH, "PLECS User Manual Version 3.6," 14 Nov. 2014. [Online]. Available: <http://www.plexim.com>
- [27] M. Musallam and C.M. Johnson, "An efficient implementation of the rainfall counting algorithm for life consumption estimation," *IEEE Trans. Reliability*, vol. 61, no. 4, pp. 978–986, Dec. 2012.
- [28] A.T. Bryant, P.A. Mawby, P.R. Palmer, E. Santi, and J.L. Hudgins, "Exploration of power device reliability using compact device models and fast electrothermal simulation," *IEEE Trans. Ind. Appl.*, vol. 44, no. 3, pp. 894–903, May 2008.
- [29] H. Huang and P.A. Mawby, "A lifetime estimation technique for voltage source inverters," *IEEE Trans. Power Electron.*, vol. 28, no. 8, pp. 4113–4119, Aug. 2013.
- [30] K. Ma, M. Liserre, F. Blaabjerg, and T. Kerekes, "Thermal loading and lifetime estimation for power device considering mission profiles in wind power converter," *IEEE Trans. Power Electron.*, vol. 30, no. 2, pp. 590–602, Feb. 2015.